Platinum and Rhodium in Tagus Estuary, SW Europe: sources and spatial distribution

Carlos Eduardo Monteiro[1,2*], Margarida Correia dos Santos[2], Antonio Cobelo-Garcia[3], Pedro Brito[1] and Miguel Caetano[1]

[1] IPMA—Portuguese Institute of Sea and Atmosphere, Division of Oceanography and Marine Environment, Av. Brasília, 1449-006 Lisbon, Portugal

[2] Environmental Biogeochemistry, Centro de Química Estrutural, Instituto Superior Técnico, Universidade de Lisboa, Av. Rovisco Pais 1, 1049-001, Lisboa, Portugal

[3] Bioxeoquímica Mariña, Instituto de Investigacións Mariñas IIM-CSIC, Eduardo Cabello 6, 36208 Vigo, Pontevedra, Spain

*Corresponding author: Carlos E. Monteiro:
carlos.monteiro@ipma.pt
carlos.e.monteiro@tecnico.ulisboa.pt

IPMA—Instituto português do Mar e da Atmosfera, Divisão de Oceanografia e Ambiente Marinho,
Av. Brasília, 1449-006 Lisboa, Portugal

+351 218 447 000

Centro de Química Estrutural, Instituto Superior Técnico, Universidade de Lisboa, Av. Rovisco Pais 1, Torre Sul Lab 11.6-2, 1049-001, Lisboa, Portugal

+351 218 419 177

ABSTRACT:

The spatial distribution of Pt and Rh was assessed in Tagus estuary and their sources discussed. Both elements were analysed in superficial sediment samples (n = 72) by adsorptive cathodic stripping voltammetry. Concentrations varied within the following ranges: 0.18 – 5.1 ng Pt g^{-1} and 0.02 – 1.5 ng Rh g^{-1}. Four distinct areas were established: "reference"; waste- and pluvial waters discharge; motorway bridges and industrialised areas. The calculated reference median concentrations were 0.55 ng Pt g^{-1} and 0.27 ng Rh g^{-1}. Linear relationships were found between Pt and Al, Fe and LOI, whereas Rh depicted scattered patterns. The highest concentrations were found nearby industrialised areas and a motorway bridge, corresponding to the enrichment of 10 and 6 times the background of Pt and Rh, respectively. The main sources of contamination to the Tagus estuary derived from historical and present industrial activities and from automotive catalytic converters. Large variations of Pt/Rh ratio (0.48–39) point to different sources, reactivity and dilution effects.

Keywords

Platinum-group elements

Spatial distribution

Superficial sediments

Tagus estuary

Anthropogenic contamination

25 **Introduction**

26

27 Technology-critical elements (TCE) are contaminants of environmental concern due to
28 increasing use in several technology-based sectors. Platinum-group elements (PGE) are
29 part of the TCE and include platinum (Pt), palladium (Pd), rhodium (Rh), iridium (Ir),
30 osmium (Os) and ruthenium (Ru). Their global demand continues to rise despite the ultra-
31 trace concentrations found in the earth's upper continental crust (UCC) (Taylor and
32 McLennan 1995; Peucker-Ehrenbrink and Jahn 2001; Ravindra et al. 2004).

33 Anthropogenic emissions of PGE have been largely attributed to the extensive use in
34 automotive catalytic converters (ACC) (European Comission 1991; Kašpar et al. 2003).
35 Platinum and Rh are included onto the ACC in the metallic or oxide forms. Due to
36 degradation and mechanical abrasion during vehicle operation, they are released into the
37 environment as fine grained particulate material (Ely et al. 2001; Moldovan et al. 2002;
38 Ek et al. 2004; Rauch et al. 2002; Prichard and Fisher 2012; Zereini and Wiseman 2015).
39 Regardless the emission rates of ng *per* kilometre *per* car (Ely et al. 2001), it has been
40 observed the increase of Pt and Rh concentrations in road dust and roadside soils reaching
41 up to 3 orders of magnitude of their crustal abundance (UCC: 0.5 ng Pt g^{-1} and 0.06 ng
42 Rh g^{-1} (Taylor and McLennan 1995; Peucker-Ehrenbrink and Jahn 2001; Zereini and
43 Wiseman 2015). The mass Pt/Rh ratio is often used to track different sources of Pt and
44 Rh. In particular, the typical range for ACC emissions varies between 5 – 16 (Ely et al.
45 2001; Ravindra et al. 2004; Rauch and Peucker-Ehrenbrink 2015). Additionally, shifts in
46 the ratio may point to inputs of industrial activities and hospital effluents to the
47 environment (Laschka and Nachtwey 1997; Rauch and Peucker-Ehrenbrink 2015).

48 The increase of PGE concentrations in urban environments has been documented over
49 the past years (Ek et al. 2004; Rauch et al. 2005, 2006; Zereini et al. 2004, 2007; Wiseman
50 and Zereini 2009; Mihaljevič et al. 2013; Rauch and Peucker-Ehrenbrink 2015; Ruchter
51 and Sures 2015; Wiseman et al. 2013, 2016; Birke et al. 2017). Studies dealing with
52 spatially-resolved distribution provide useful information in the assessment of potential
53 contamination sources to the aquatic systems. These studies in estuaries are mainly
54 focused in Pt (Terashima et al. 1993; Wei and Morrison 1994; Cobelo-García et al. 2011,
55 2013; Zhong et al. 2012) and very scarce information exists for Rh (e.g. Essumang et al.
56 2008). Most of the works focused on Rh center their research only in restricted areas or
57 samples of estuarine systems (e.g. Essumang et al. 2008; Almécija et al. 2016a). Thus,
58 the very limited research of Pt and Rh spatial distribution in river-estuarine systems exists
59 to overcome the sinks and sources of these elements. We hypothesised that Pt and Rh
60 contamination in Tagus estuary could be imprinted in superficial sediments because of
61 the anthropogenic pressures and hydrodynamic of the estuary. Thus, we aimed (1) to
62 quantify Pt and Rh concentrations in superficial sediments of the Tagus estuary; (2) to
63 assess the influence of anthropogenic sources loading into the sediments; and (3) to define
64 baseline patterns for future monitoring studies envisaging unknown PGE emissions to
65 this aquatic system.
66

67 **Material and methods**

68

69 Study area

70

71 Estuaries are very important in the interchange of mass between the land and the ocean.
72 The Tagus estuary (Fig. 1) is one of the largest in western Europe, with approximately
73 320 km^2 comprising small islands, sand banks, and intertidal mudflats that account for
74 ~40% of the total area. The inner bay has approximately 25 km long and 15 km wide, and
75 the bathymetry ranges between 0 and 7 meters' depth. Downstream, a narrow channel
76 reaching 47 m depth and 2 km wide connects the estuary to the Atlantic Ocean (Fortunato
77 et al. 1999; Freire et al. 2007; Taborda et al. 2009; Vaz et al. 2011).

78 The freshwater input to the Tagus estuary depends on rain events and it has its origin
79 mainly from the Tagus river (350 $m^3 s^{-1}$, average annual flow), as well as from other small
80 tributaries (< 35 $m^3 s^{-1}$). The water circulation in Tagus estuary is mainly tidally driven,
81 often considered mesotidal and vertically well-mixed (Vaz et al. 2011). Resuspension of
82 particulate matter from sediments over the tidal cycling can occur due to wind forcing,
83 rising tide, and water exchange with the main channels (Vale and Sundby 1987; Freire et
84 al. 2007). Particle's settling occurs during the turnover of tides, depending on the current
85 velocity and bathymetry. The particle resuspension-settling cycles in each semi-diurnal
86 tide may play a key role on the scavenging of Pt and Rh to the sediments.

87 The Tagus estuary is well characterised with respect to the hydrodynamics (e.g. Vale and
88 Sundby 1987; Fortunato et al. 1999; Vaz et al. 2011), trace elements (Vale et al. 2008;
89 Santos-Echeandía et al. 2010; Caçador et al. 2012; Monteiro et al. 2016), persistent
90 organic pollutants (Gil and Vale 1999; Mil-Homens et al. 2016), and nutrients (Cabeçadas
91 1999; Cabrita et al. 1999; Mateus and Neves 2008). For PGE, only data on Pt, Rh and Os
92 were reported before in spot areas of the estuary and coastal sediments (Cobelo-García et
93 al. 2011; Almécija et al. 2015, 2016a, 2016b), pointing to anthropogenic inputs. The
94 Tagus estuary (Fig. 1) has particular features that makes it a natural setting for the study
95 of these elements. The anthropogenic pressures result from heavily industrialised areas,

with historical and present-day activities. At the southern margin exits a metallurgic complex (SN), a chemical complex (BRR) with a large area decommissioned, and an inactive shipyard (LN). At the northern margin operates a chemical industrial unit (CN) and the denser urban area is settled. Intense urban sprawl reaches 2.8 million of inhabitants around the estuary (Costa 2016) with several Waste Water Treatment Plants (WWTP) and pluvial water drainage channels dispersed in the margins. Three major WWTP exist in the northern margin: Alcântara (A), Beirolas (B) and Chelas (C); and at Terreiro do Paço (TP) is located one of the main channels for the pluvial runoff. Moreover, the Tagus estuary is crossed by two high traffic motorway bridges, Vasco da Gama (VG bridge) and 25 de Abril (25A bridge), where 175000 – 225000 vehicles pass every day (IMT 2016).

Sediment samples collection and preparation

Taking into account potential sources of Pt and Rh to the Tagus estuary, superficial sediment samples (< 5 cm depth) were collected in 72 stations on-board of a small vessel using a Van Veen grab sampler. A set of samples (n = 12) was collected in 2015 at the waste- and pluvial waters effluents (A, B, C and TP, in Fig. 1). In addition, two control samples were collected upstream (-U) and downstream (-D) of each effluent, spaced by approximately 0.5–1 km. Another set of superficial sediments (n = 60) was sampled in June 2016, following a spatial grid covering the immersed area of the estuary. Emphasis on VG bridge influence area was preferred since it was not feasible to collect samples nearby 25A bridge, due to the higher current velocity and coarser sediments (rocks, gravel and coarse sand) than in the rest of Tagus estuary (Fig. 1).

120 Sediment samples were dried in an oven at 40 ^{0}C. After homogenisation, aliquots were
121 separated for grain size analysis and after sieving (< 2 mm) another portion was ground
122 to a fine powder for further analyses.

123

124 Analytical procedures

125

126 Material and chemicals

127

128 All laboratory material used was acid-cleaned by successive immersion periods of 48
129 hours in ~20 % nitric acid (HNO_3) followed by ~20 % hydrochloric acid (HCl).
130 Afterwards, the material was rinsed with Milli-Q water (18.2 MΩ.cm, 25 ºC) and let to
131 dry in a clean room. All reagents used throughout the work were always of high-purity
132 grade, either for samples digestion or analysis: hydrofluoric acid (HF) 40 %, HNO_3 65 %
133 and HCl 30 % (*Suprapur*, Merck), sulphuric acid (H_2SO_4) ≥ 95 % (*Trace*SELECT,
134 Fluka), hydrazine sulphate (HZ; p.a., Fluka) and formaldehyde 13 M (FA 36.5 %, Riedel-
135 de-Haen). Diluted standards of 1.0 µg Pt L^{-1} and 1.0 µg Rh L^{-1} in 0.1 M HCl were weekly
136 prepared from standard solutions of Pt and Rh 1000 mg L^{-1} (*Trace*CERT, Fluka). Other
137 solutions were prepared in Milli-Q (18.2 MΩ.cm) water and kept in perfluoroalkoxy
138 flasks.

139

140 Grain size and Loss on Ignition

141

142 Grain size analysis was carried out in sediments by dry sieving (Gaudêncio et al. 1991).
143 According to Folk (1954), three classes of sediment grain sizes (%) were used to evaluate
144 the contents of gravel (≥2 mm), sand (2 – 0.063 mm), and the finer fraction corresponding
145 to silt and clay (< 0.063 mm). Organic matter was determined on the basis of Loss-on-
146 Ignition (LOI, in %), estimated by the weight difference of dried samples at 105 ^{0}C and
147 heated at 450 ^{0}C in a muffle furnace for 2 h (Craft et al. 1991). The temperature used in
148 this procedure ensures that the sediment carbonate fraction was unchanged.

149

150 Major elemental composition

151

152 Major elemental composition of the sediments (total Al, Fe, Mn, Mg and Ca) was
153 quantified in ≈0.1 g (dry weight, d.w.) aliquots after a two steps digestion. Complete
154 dissolution was achieved using a mixture of 1 mL of *aqua regia* (a mixture of HCl:HNO_3;
155 3:1) and 3 mL of HF (40%), at 100 ^{0}C for 1 h in closed Teflon autoclaves (Loring and
156 Rantala 1992). The resultant solution was evaporated to near dryness in Teflon vessels
157 (DigiPrep HotBlock-SCP Science), re-dissolved with 1 mL of distilled HNO_3 and 5 mL
158 of Milli-Q water, heated for 20 min at 75 ^{0}C and diluted in Milli-Q water to a final volume
159 of 50 mL (Caetano et al. 2009). Inductively coupled plasma – mass spectrometry (ICP-
160 MS) was used to determine major elemental composition of the sediments. The
161 determinations were done in quadrupole ICP-MS from Thermo Elemental (X-Series),
162 equipped with a concentric Meinhard nebulizer and a Peltier impact bead spray chamber,
163 following the procedure previously reported Brito et al. (2018). Main experimental
164 parameters were as follows: forward power 1400 W; peak jumping mode; 150 sweeps per
165 replicate; dwell time of 10 ms; dead time of 30 ns.

166

167 Pt and Rh determination

168

169 For the determination of Pt and Rh in the sediments the procedures of Nygren et al. (1990)
170 and of Haus et al. (2009) were followed for samples digestion. Sediment samples of ≈0.2
171 g of each were heated in quartz crucibles up to 800 ºC in a muffle furnace. After cooling,
172 samples were transferred to PFA pressurised digestion vessels (MarsXpress, CEM) and
173 they were microwave-assisted digested in the presence of 4 ml of *aqua regia*. Afterwards,
174 samples were evaporated to near dryness at 85 ºC in a hot plate, re-dissolved in 1 mL of
175 H_2SO_4, and were left to evaporate the residual acids until constant volume. Finally the
176 residue was transferred to polypropylene Digitubes (SCP Science) and diluted to 25 mL
177 in 0.1 M HCl. Adsorptive Cathodic Stripping Voltammetry (AdCSV) was used for the
178 determination of Pt and Rh, following the procedure optimised by Monteiro et al. (2017).
179 Briefly, the voltammetric measurements were carried out in an acclimatized room at 25
180 ± 2 ºC. A potentiostat/galvanostat from ECO Chemie, Autolab PGSTAT 128N
181 (Metrohm), was used as the source of the applied potential and as the measuring device,
182 connected to the Metrohm Stand 663. A conventional three-electrode configuration was
183 used: a Static Mercury Drop Electrode (SMDE) as the working electrode, an
184 $Ag/AgCl/KCl_{(sat)}$ as the reference electrode (placed inside a salt bridge with 3 M KCl)
185 and a carbon rod as auxiliary electrode. The whole system was controlled and data
186 analyzed with the GPES v4.9 software (EchoChemie). The standard addition method was
187 used to quantify Pt and Rh concentrations (Monteiro et al. 2017). All measurements were
188 done at least in triplicate.

189

190 Quality control of the analytical procedures

191

192 The quality control on major elements determination was assessed by running a multi-
193 element solution in every 10 samples. Coefficients of variation for metal counts (n = 3)
194 were < 2 %. Certified reference materials (CRM) MAG-1, G-2, and BHVO-1 (USGS),
195 with different matrices, were used to control the analytical procedure. The results
196 obtained did not differ significantly ($p > 0.05$) from the certified values. Procedural blanks
197 always accounted for < 1 % of total concentrations in samples (Brito et al. 2018).

198 For Pt and Rh determinations, the accuracy was evaluated through the recoveries (%) in
199 digested CRM road dust BCR-723 (EC-JRC-IRMM). Recoveries were 92 ± 11 % for Pt
200 and 85 ± 13 % for Rh (n > 10), which were within the certified ranges. Procedural blanks
201 (n > 10) were analysed to evaluate potential cross contamination. The average limits of
202 detection were 0.012 ± 0.005 ng Pt g^{-1} and 0.013 ± 0.005 ng Rh g^{-1} (n > 10). Further
203 details are fully described in Monteiro et al. (2017).

204

205 Data processing

206

207 All statistical analysis was performed using XLSTAT (Addinsoft). Normality of the data
208 was assessed using the Shapiro–Wilk test. Since most of the variables did not present
209 normal distribution, non–parametric Kruskal–Wallis (H) test was applied to assess the
210 differences in median values, with post hoc test. In addition, Mann-Whitney (U) test was
211 also applied to assess significant differences between groups. Grubbs test was used to

212 check the data for outliers. In addition, Spearman rank correlations (r_S) were also
213 computed to evaluate trend relationships (Miller and Miller 2010).

214 Images of the spatial distributions were generated using the Ocean Data View software
215 (ODV; Schlitzer 2017) using Data Interpolating Variational Analysis (DIVA) method.
216 This method takes into account topographic and dynamic constraints when generating
217 grids based on a relative low number of observations (Troupin et al. 2012). However,
218 boundary conditions were superimposed in ODV/DIVA by delimiting the area of interest
219 of the Tagus estuary, with better resolution in the rough edges of the estuary in order to
220 improve interpolations.

221

222 **Results**

223

224 Characterisation of superficial sediments

225

226 Sediment samples from Tagus estuary were characterised for grain-size, LOI and major
227 elemental composition. Descriptive statistics of the data are summarised in Table 1. The
228 median value of the sand fraction (2 – 0.063 mm) was 41 % and in general lower than the
229 fine-sized fraction (< 0.063 mm) that corresponds to silt and clay material (Table 1). The
230 contents of Al, Fe, and LOI ranged up to ~10 %, and the higher levels were associated
231 with deposits of fine-grained material in the northern margin and mudflats of the upper
232 and middle estuary. Magnesium and Mn were below 1.4 and 0.71 %, respectively, with
233 no clear distribution pattern within the estuary. Calcium ranged up to 7.1 % and the
234 highest concentrations were found in samples containing fragments of bivalve shells.

235

236 Concentrations and spatial distribution of Pt and Rh

237

238 The concentrations of Pt and Rh in superficial sediments from the Tagus estuary varied
239 between 0.18 – 5.1 ng Pt g^{-1} and 0.02 – 1.5 ng Rh g^{-1} (d.w.) (Fig. 2), being the median
240 values 0.60 ng Pt g^{-1} and 0.54 ng Rh g^{-1} (Fig. 3a).

241 Based on the potential sources to the estuary and spatial distribution of both elements,
242 four estuarine sections were outlined for further discussion (Fig. 3): (*i*) "*reference*
243 *concentration"* of Pt and Rh that comprises the stations distant from potential sources;
244 (*ii*) *waste- and pluvial waters discharge sites* in the northern margin; (*iii*) *motorway*
245 *bridges*, in particular *VG bridge*; and (*iv*) *industrialised areas*, corresponding to sites
246 BRR, SN, LN and CN. Differences on median values among groups were observed, being
247 significantly different for Pt ($H(3, n=72) = 20.30$, $p<0.001$) and for Rh ($H(3, n=72) =$
248 7.867, $p<0.05$). When comparing paired– sections (Mann-Whitney (U) test), the industry
249 section was significantly different from the other sections ($p<0.05$) (Fig. 3b) in the case
250 of Pt. Although at VG bridge have been found higher values up to 6 times than in WWTP
251 and reference sections, the broad interval of variation lead to no significant differences
252 between sections ($p>0.05$). In the case of Rh, no significant differences were found
253 between the reference, WWTP and industry sections ($p>0.05$) (Fig. 3c). Other statistical
254 similarities found were those of WWTP section with VG bridge and industry sections
255 ($p>0.05$) and between VG bridge and industry sections ($p>0.05$). However, the lack of
256 statistical differences for Rh between industry and the other sections is largely dependent
257 on the low concentrations found at BRR than in the other industrial sites (Fig. 3d).
258 Nonetheless, their environmental significance should not be disregarded.

Reference levels in Tagus estuary

The lowest concentrations of Pt and Rh, up to the median values, were found mostly in the central areas of the estuary. Considering only the stations far from possible anthropogenic sources as reference stations, levels of Pt ranged from 0.18 – 1.5 ng g^{-1} (d.w.) with a median of 0.55 ng g^{-1}. For Rh concentrations varied within 0.02 – 1.3 ng g^{-1} (d.w.) with a median of 0.27 ng g^{-1}.

It was found in those stations a clear affinity of Pt for Al, Fe and LOI, with significant regressions (Fig. 4). When normalised, the spatial distribution of Pt/LOI and Pt/Fe (Fig. 5) resulted in a wider spread of Pt signature than that observed for Pt/Al. No significant correlations ($p>0.05$) were found between Rh concentrations and the content of Al, Fe and LOI (Fig. 4).

Waste- and pluvial waters discharge

Relatively low concentrations of Pt and Rh were observed in the discharge sites of waste- and pluvial waters at the northern margin (A, B, C and TP, in Fig. 1). Concentrations of both metals were closer to the reference levels of the Tagus estuary, ranging from 0.23 – 1.0 ng Pt g^{-1} and 0.22 – 0.98 ng Rh g^{-1} (d.w.). However, when concentrations were normalized to Al or LOI, sediment levels from the discharge sites of Alcântara (A) and Beirolas (B) WWTP were higher than the values found in upstream and downstream control stations (A-U, B-U and A-D, B-D, respectively; Fig. 6). This trend was not found

for WWTP of Chelas (C) and the pluvial waters discharge site at Terreiro do Paço (TP), presumably due to their low discharge into the estuary.

Anthropogenic point sources and signature in sediments

Concentrations of both elements increased downstream of the VG bridge and in both margins closer to the bridge ends, varying from 0.22 – 3.0 ng Pt g^{-1} and from 0.12 – 1.1 ng Rh g^{-1} (d.w.). Furthermore, the highest levels were found closer to the industrialised areas (Fig. 3 and S.I. Fig. 1). Platinum concentrations (d.w.) were 1.8 ng g^{-1} at LN, 2.5 ng g^{-1} at SN, 2.7 ng g^{-1} at CN and up to 3.5-5.1 ng g^{-1} at BRR sites. Regarding Rh levels, they varied between 1.2 and 1.5 ng g^{-1} at LN, SN and CN, but lower values were found at BBR, <0.01 – 0.13 ng g^{-1}.

In the Tagus estuary, Pt/Rh ranged within 2 orders of magnitude, between 0.48 and 39 (Fig. 7). The lowest Pt/Rh ratio corresponded to the reference signature, varying between 0.48 and 4.0 and with a median value of 1.6 (all reference stations). If it is only considered the innermost stations of the Tagus Natural Reserve area, where no direct anthropogenic activities exist, then the range of Pt/Rh decreases to a median value of 0.9. Similar to that reference value, the signature of particles derived from the WWTP stations was low (0.6 – 1.6). In sediments closer to VG bridge, values were in general higher than the reference section (0.9), ranging from 0.5 to 5.6. Additionally, a road dust sample was collected in a dense traffic road, containing 551 ng Pt g^{-1} and 84 ng Rh g^{-1}, which corresponds to Pt/Rh of 6.6. The largest difference on Pt/Rh mass ratio (1.5 – 39) was observed in industrialised areas. At BRR it was found the highest Pt/Rh values (25 – 39), while in other industrial sites Pt/Rh values were low (1.5 – 2).

306

307 **Discussion**

308 The reference value of Pt concentration in Tagus estuary (0.55 ng g^{-1}) is similar to the
309 concentration in the Upper Continental Crust (UCC, 0.5 ng Pt g^{-1}; Taylor and McLennan
310 1995; Peucker-Ehrenbrink and Jahn 2001; Ravindra et al. 2004). Furthermore, that value
311 is comparable to the baseline concentration in shelf sediments of the Tagus in the
312 sediment horizon corresponding to 1920, found by Cobelo-Garcia et al. (2011). This was
313 not found for Rh since the estimated reference level in Tagus estuary sediments (0.27 ng
314 g^{-1}) was 4 times higher than the value indicated for the UCC (0.06 ng Rh g^{-1}; Taylor and
315 McLennan 1995) and also for the deepest layers of a salt marsh core, reported by Almécija
316 et al. (2016a). The concentrations of Pt in Tagus estuary sediments (0.18 – 5.1 ng g^{-1}) are
317 in the range of those reported by Zhong et al. (2012) for the Pearl River estuary, China,
318 Wei and Morrison (1994) for three urban river sediments in Gothenburg, Sweden, and
319 Prichard et al. (2008) in Humber estuary, UK. However, levels of this element in Tagus
320 are lower than those found by Ruchter and Sures (2015) in the river Alb, Germany (up to
321 45 ng Pt g^{-1}) or by Sutherland et al. (2015) in the bed sediments of Nuuanu stream, Hawaii
322 (5.8 – 40 ng Pt g^{-1}). The range of Rh concentrations determined in Tagus sediments (0.02
323 – 1.5 ng g^{-1}) is comparable to those reported by Sutherland et al. (2015) for in Hawaii
324 (0.32 – 3.5 ng g^{-1}) or by Prichard et al. (2008) for the Humber estuary, UK (1 – 2 ng g^{-1}).

325

326 *Variation of the reference levels in the estuary*

327

328 Low concentrations of Pt and Rh were observed in the central areas of the Tagus estuary,
329 ranging from 0.18 – 1.5 ng Pt g^{-1} and 0.02 – 1.3 ng Rh g^{-1} (d.w.). In order to minimize the

330 anthropogenic contributions of these elements (Dung et al. 2013), the variation of Pt and
331 Rh in reference stations was assessed in sediments far from potential sources by
332 evaluating the relationships with the ancillary parameters. Aluminium content is usually
333 used due to the conservative behaviour and rare anthropogenic inputs, being a proxy for
334 particle's nature in sediments (Loring and Rantala 1992; Matys Grygar and Popelka
335 2016). However, using Al-normalised metal concentrations is not straightforward and
336 other parameters may be used, like Fe and organic matter (Matys Grygar and Popelka,
337 2016). The affinity of Pt towards Al, Fe and LOI indicates that its distribution in
338 sediments is governed by the sediment characteristics or by a group of several parameters,
339 contrarily to Rh. A clear affinity of Pt to the fine-sized fraction (silt and clay) of the
340 sediments was observed, but not for Rh. Thus, the transport of Pt and Rh within the
341 estuary is likely to be differently affected by the nature of particulate material in
342 association with the hydrodynamic regime of the estuary.

343 Different contribution of both margins on the sediment loadings is due to geologic
344 features and intense, yet dissimilar, anthropogenic pressures (Taborda et al. 2009). The
345 reference levels of Pt and Rh in the Tagus estuary may derive from weathering of Neo-
346 Cretaceous basalts and pyroclasts from the Lisbon Volcanic Complex (Prudêncio et al.
347 1993; Taborda et al. 2009). The higher contribution yielded by the southern margin
348 sediments includes sandstones, sand, gravel, silt and clay from detrital Plio-Pleistocene
349 that constitute the fluvial terraces, resulting mainly from erosion (Taborda et al. 2009). In
350 addition, pyrite is the main group of minerals responsible for a background signature of
351 PGE. However, the reference levels may be influenced by specific anthropogenic
352 activities in the Tagus, such as different types of industry. The implementation of a
353 chemical plant in the southern margin of the estuary that operated during the XX century
354 (1909-1990s) included a pyrite-roasting unit and a smelter. During this period, the

355 industry used pyrite from Lousal and Aljustrel mines, both part of the Iberian Pyrite Belt
356 (Mil-Homens et al. 2013). This raw material was stored in large piles in the southern
357 margin of the estuary and could cause the spread of particulate material containing PGE
358 in a large area, including the estuary. Thus, the input of this geological material for such
359 a long period could mask the background Pt and Rh values existing in the original
360 minerals from the Tagus river basin.

361

362 Sources and distribution of Pt and Rh

363

364 *Waste- and pluvial waters discharge sites*

365

366 The concentrations of Pt and Rh found in sediments closer to the WWTP outfalls were
367 within the range of reference levels in Tagus estuary. However, the increased signal in
368 stations A and B, after normalization to Al and/or LOI, reflects the drainage of a large
369 urban area for a considerable period of time, from Lisbon, which mainly includes
370 domestic and hospital effluents, and pluvial runoff. The presence of Pt-based anticancer
371 drugs was recently reported in sewage and wastewaters (Vyas et al. 2014). These authors
372 did not find evident relationships between the administered quantities of Pt and measured
373 concentrations in drainage, reflecting the randomness of the excreted Pt. Furthermore,
374 Monteiro et al. (2017) showed that an increase in dissolved Pt concentrations was detected
375 in the effluents of the WWTP. During the water treatment along the WWTP, dissolved Pt
376 concentrations reduced to half while dissolved Rh was kept invariable. Although low
377 dissolved concentrations of Pt and Rh (ng L^{-1}) are introduced in the estuary through the
378 WWTP, the input of high volume of water (3 – 100 m^3 s^{-1}) results in a detectable imprint

379 in sediments (ng g^{-1}). Furthermore, coupling other elements with Pt or Rh can be of major
380 interest to track anthropogenic emissions of technology-critical elements. In fact, rare
381 earth elements (REE) do support the transfer of urban contamination from different
382 anthropogenic sources into the Tagus estuary. Brito et al. (2018) observed this signature
383 for some of the REE at the same WWTP stations, e.g. Gd (S.I. Fig. 2) and Ce, which
384 suggests the association of metals to the particulate load from urban effluents and runoff
385 material. Despite having distinct point sources, their pathways into the estuary are in
386 general the same. Along with Pt, Gd can be used to track anthropogenic contamination
387 with source in medical applications (Ebrahimi and Barbieri, 2019). In addition, Wiseman
388 et al. (2016) used Ce coupled to Pt, Rh and Pd to evaluate ACC emissions in roadside
389 soils from Toronto, Canada.

390

391 *Motorway bridges*

392

393 Both Pt and Rh followed the same spatial distribution pattern with increasing levels
394 downstream of VG bridge. Furthermore, a clear input was also found in the north margin
395 at the bridge end. These results point that both elements have the same anthropogenic
396 source, with these signatures of Pt and Rh most likely resulting from the abrasion and
397 degradation of ACC. This particular spatial distribution may derive from the concrete
398 structure of the VG bridge. The road dust material accumulates along the bridge during
399 the dry season and then is flushed directly to the estuary during rain periods through a
400 system of gully pots. The road dust enters the estuary at several points located along the
401 bridge and is spread according to the tidal and hydrodynamic regime. The spreading of
402 road dust enriched in Pt and Rh downstream the bridge results from the ebb and flushing

403 semidiurnal cycles. The bridge is located approximately in the maximum turbidity zone
404 of the estuary and major mixture of freshwater and seawater occurs towards the estuary
405 mouth. In a previous study, Almécija et al. (2016b) found elevated concentrations of Pt
406 (40 ng g^{-1}) in surface sediments from a system of channels and creeks in a salt marsh at
407 the southern margin. In these ecosystems, particulate material including road dust is
408 retained by halophyte plants and deposited in low hydrodynamic areas.

409 It should be pointed out that it was not feasible to collect samples in the surroundings of
410 25A bridge. Low sedimentation rate in the bridge area is due to the narrow connection to
411 the sea, where higher depth (up to 47 m) and current velocity (up to 2.0 m s^{-1}) are observed
412 than in the rest of the estuary, and the nature of bottom substrate is mainly rock gravel.
413 These characteristics coupled with the bridge structure do not favour a localised
414 deposition site. This bridge has a gridded metallic deck that allows rainwater and road
415 dust particles to pass through, without a channelled drainage system. It has a navigation
416 clearance height of 70 m above the water level in comparison with the 14 m of VG bridge.
417 Thus, 25A bridge it is more exposed to environmental conditions than VG bridge, such
418 as strong winds. All these characteristics result in a wider spread of road dust. Therefore,
419 it is hypothesised that no clear signatures of Pt and Rh from this source could be found in
420 sediments.

421 The input of both elements through the motorway bridges can be estimated based on
422 traffic and structural characteristics. It is noteworthy that regardless the higher traffic
423 density in 25A bridge, three times higher (≈150 000 cars d^{-1}) than in VG bridge, Pt and
424 Rh estimated emissions from ACC were lower. The estimated total emissions since the
425 opening of VG bridge in 1998 ranged from 542 – 937 g of Pt and 130 – 262 g of Rh.
426 Furthermore, if we calculate Pt emissions per year on VG bridge, we found that our lower
427 value is ≈30 g Pt y^{-1} (542 g Pt /18.1 years), which is comparable to the ≈33 g Pt y^{-1} (450

g Pt /13.6 years) estimated by Almécija et al (2015) using the same approach. This estimation may vary due to the different sedimentation rates found along the ~17 km of the VG bridge that crosses the larger section of the Tagus estuary. For the 25A bridge a lower interval of emissions was found, 171 – 312 g of Pt and 41 – 87 g of Rh (further details in S.I. Table A-1). Even with higher vehicle traffic on 25A bridge than in VG bridge, it is clear that their extension plays a major role in the estimated emissions of Pt and Rh from ACC.

Industrialised areas

The levels of Pt and Rh at stations BRR, SN, LN, and CN (circles in Fig. 1) point to local anthropogenic sources. The concentrations correspond to an increase up to 10 (Pt) and 6 (Rh) times the reference levels estimated in the estuary.

The increase of Pt in BRR superficial sediments may suggest a recent point source, which could be explained by the current production of fertilizers or the historical slags in the area exposed to the atmospheric conditions. The chemical-industrial complex at BRR had a long history in the production of nitric and sulphuric acids, and fertilizers, which may have used Pt as catalyst (e.g. Hatfield et al. 1987), with peak activity around the 1960s and early 1970s. The pyrite ore processing used to extract Cu, Pb, Au, and Ag, may have also contributed to that increase. The particulate material from the exposed piles of pyrite slag could be transported easily into the estuary through the air or drainage channels in the margin. However, Rh concentrations were very low. Metal contamination patterns from BRR industrial activities were previously reported for Hg (Canário et al. 2005), Cd,

Pb, Ni and As (Vale et al. 2008), and more recently for the YREE, e.g. Y (Brito et al. 2018). Thus, BRR site may be a hotspot for PGE and further research is ongoing.

Part of the slag at BRR was transferred to another industrial complex and used as raw material in metallurgical industry. This unit located also in the southern margin of the Tagus (SN site) continues to operate producing steel and treating slag residues. At this unit, the increased Rh concentrations suggest that Rh was more mobilized to the aquatic environment compared to Pt.

Another anthropogenic source of both PGE was found at the LN site, currently a dismantled shipyard but fully operating in the 1960s and early 1970s. By that time, 30 % of the world tanker fleet was repaired in this shipyard that included a variety of iron and steel works, releasing large amounts of metallic residues. The former activity coupled with the remaining of such large and abandoned infrastructures could be responsible for the Pt and Rh input to the sediments. Considering the peak activity of the chemical-industrial complex at BRR and the shipyard at LN, Pt and Rh emitted to the Tagus estuary must have been larger than those estimated in this study. The industrial activity at BRR decreased after dismantling the acid production and pyrite processing units almost two decades ago. Thus, levels in superficial sediments suggest continuous input from the fertilizer unit currently operating and/or mobility of Pt within the sedimentary column.

In the northern margin, Pt and Rh concentrations found at the CN site are likely related to the chemical industry operating for more than half of a century. A chlor-alkali industry uses a catalytic hydrogenation process based on PGE non-supported or supported catalysts (e.g. on silica or alumina; Paparatto et al. 2010; Lemaire et al. 2014). The degradation of the catalyst releases Pt and Rh that may reach the estuary through the industrial effluent. The narrow estuary channel where this unit is located has lower current

475 velocity and higher sedimentation rates, which favours the deposition of Pt and Rh in
476 bottom sediments. Furthermore, the concentration of Rh found at CN site was the highest
477 in the entire estuary, suggesting its use as a catalyst, as well as Pt. Moreover, relatively
478 high concentrations of some of the REE were also observed at this site (Brito et al. 2018).
479 In addition to the previously reported contamination by Hg (Cesário et al. 2016), Pt, Rh
480 and REE underpin the industrial point sources of contamination in Tagus estuary.

481

482 *Signature of Pt and Rh in sediments*

483

484 Platinum and Rh sources are often assessed through the Pt/Rh mass ratio (e.g. Sutherland
485 et al. 2015). This ratio variability relies on different sources, such as industrial or hospital
486 effluents than on changes of ACC's composition (Ruchter et al. 2015). Biogeochemical
487 processes in the water column or in bottom sediments may also affect Pt and Rh
488 differently due to their different reactivity (Jarvis et al. 2001). Lower Pt/Rh values
489 obtained on reference stations do not strictly represent a background because of the
490 atmospheric input of material and tidal transport of particles from other estuarine areas.
491 By shifting the concentration of one element, either Pt or Rh due to an additional source,
492 this mass ratio can vary considerably. In WWTP section, the low values found may
493 suggest that Pt signature derived from hospital and domestic effluents may be masked by
494 dilution from the drainage system and/or additional Rh sources, such as those from ACC.

495 In sediments closer to VG bridge, Pt/Rh reflect mainly the ACC contribution. This section
496 presented larger variations in the Pt/Rh ratio, having values within the typical range
497 reported for ACC (Ely et al. 2001; Ravindra et al. 2004; Rauch and Peucker-Ehrenbrink
498 2015). Additionally, the road dust sample collected in a dense traffic road presented Pt/Rh

499 mass ratio of 6.6.Thus, the variable Pt/Rh signature in sedimentary material closer to the
500 VG bridge indicates that different dilution/concentration effects masking the real ACC
501 signature may occur. At the estuary margins, around the VG bridge, a dilution effect exists
502 due to the input of Pt and Rh from urban sources decreasing the signature. During the
503 transport of road dust to the estuary, the partition of Pt or Rh may change and shift the
504 ratio Pt/Rh. This suggests Pt and Rh in the Tagus estuary have a common source in ACC
505 emissions from urban areas.

506 The highest Pt/Rh mass ratio observed in BRR sediments, compared to the other industrial
507 sites (CN, SN and LN) that presented low values, is presumably related to the input of
508 material with low Rh concentrations. This suggests that the industrial source at BRR has
509 added to the estuary increased levels of Pt in comparison to Rh. At the other sites, the
510 industrial activities supplied both elements to the sediments, lowering the Pt/Rh ratio.

511

512 **Conclusions**

513

514 Platinum and Rh spatial distributions in superficial sediments of the Tagus estuary were
515 assessed and reference levels are reported. Reference levels for Pt are close to the
516 background, however Rh was ca. 5 times higher than its estimated crustal abundance. The
517 main sources of these metals were confirmed, in particular those from cars and industries
518 through their use as catalysts. Motorway bridges are a relevant via for the entrance of Pt
519 and Rh into the estuary. The extent of this contribution relies on the structural
520 characteristics and extension of the bridges. Even though, the Pt/Rh ratio found in
521 sediments does not clearly reflect that typical of automotive catalytic converters. The
522 highest contamination levels were found in industrialised areas, revealing the important

contribution of industrial activities. The magnitude of those emissions remains unclear and needs further evaluation because they may be dominant. This work stands as reference information for future studies and highlights the importance of understanding Pt and Rh biogeochemistry in hydrodynamic estuaries, for which the lack of knowledge remains. Platinum and Rh concentrations will likely increase and medium-term monitoring of those elements is recommended.

Acknowledgements

Carlos E. Monteiro (CEM) acknowledges the Portuguese Foundation for Science and Technology (FCT) for the grant funding of his PhD (SFRH/BD/111087/2015). The authors would like to gratefully acknowledge also the support of FCT projects UID/QUI/001002013 and PTDC/QEQ-EPR/1249/2014 'Recovery versus environmental impacts of Rare Earth Elements derived from human activities' (REEuse); the COST Action TD1407 - Network on Technology-Critical Elements (NOTICE) - from environmental processes to human health threats, by means of a short term scientific mission support to CEM; and the support of Rute Cesário in part of the field work and ICP-MS analysis.

References

Almécija, C., Cobelo-García, A., & Santos-Echeandía, J. (2016a). Improvement of the ultra-trace voltammetric determination of Rh in environmental samples using signal transformation. *Talanta*, *146*, 737–743. doi:10.1016/j.talanta.2015.06.032

Almécija, C., Cobelo-García, A., Santos-Echeandía, J., & Caetano, M. (2016b). Platinum in salt marsh sediments: Behavior and plant uptake. *Marine Chemistry*, *185*, 91–103. doi:10.1016/j.marchem.2016.05.009

Almécija, C., Sharma, M., Cobelo-García, A., Santos-Echeandía, J., & Caetano, M. (2015). Osmium and platinum decoupling in the environment: Evidences in

intertidal sediments (Tagus Estuary, SW Europe). *Environmental Science and Technology*, *49*(11), 6545–6553. doi:10.1021/acs.est.5b00591

Alvera-Azcárate, a., Ferreira, J. G., & Nunes, J. P. (2003). Modelling eutrophication in mesotidal and macrotidal estuaries. The role of intertidal seaweeds. *Estuarine, Coastal and Shelf Science*, *57*(4), 715–724. doi:10.1016/S0272-7714(02)00413-4

Arpentinier, P., Koenig, J., & Vlaming, R. (1998, April 8). Nitric acid production. Google Patents.

Birke, M., Rauch, U., Stummeyer, J., Lorenz, H., & Keilert, B. (2017). A review of platinum group element (PGE) geochemistry and a study of the changes of PGE contents in the topsoil of Berlin, Germany, between 1992 and 2013. *Journal of Geochemical Exploration*. doi:https://doi.org/10.1016/j.gexplo.2017.09.005

Brito, P., Prego, R., Mil-Homens, M., Caçador, I., & Caetano, M. (2018). Sources and distribution of yttrium and rare earth elements in surface sediments from Tagus estuary, Portugal. *Science of The Total Environment*, *621*, 317–325. doi:https://doi.org/10.1016/j.scitotenv.2017.11.245

Cabeçadas, L. (1999). Phytoplankton production in the Tagus estuary (Portugal). *Oceanologica Acta*, *22*(2), 205–214. doi:https://doi.org/10.1016/S0399-1784(99)80046-2

Cabrita, M. T., Catarino, F., & Vale, C. (1999). The effect of tidal range on the flushing of ammonium from intertidal sediments of the Tagus estuary, Portugal. *Oceanologica Acta*, *22*(3), 291–302. doi:10.1016/S0399-1784(99)80053-X

Caçador, I., Costa, J. L., Duarte, B., Silva, G., Medeiros, J. P., Azeda, C., et al. (2012). Macroinvertebrates and fishes as biomonitors of heavy metal concentration in the Seixal Bay (Tagus estuary): Which species perform better? *Ecological Indicators*, *19*, 184–190. doi:https://doi.org/10.1016/j.ecolind.2011.09.007

Caetano, M., Prego, R., Vale, C., de Pablo, H., & Marmolejo-Rodríguez, J. (2009). Record of diagenesis of rare earth elements and other metals in a transitional sedimentary environment. *Marine Chemistry*, *116*(1), 36–46. doi:https://doi.org/10.1016/j.marchem.2009.09.003

Cobelo-García, A., López-Sánchez, D. E., Almécija, C., & Santos-Echeandía, J. (2013). Behavior of platinum during estuarine mixing (Pontevedra Ria, NW Iberian Peninsula). *Marine Chemistry*, *150*, 11–18. doi:10.1016/j.marchem.2013.01.005

Cobelo-García, A., Neira, P., Mil-Homens, M., & Caetano, M. (2011). Evaluation of the contamination of platinum in estuarine and coastal sediments (Tagus Estuary and Prodelta, Portugal). *Marine Pollution Bulletin*, *62*(3), 646–650. doi:10.1016/j.marpolbul.2010.12.018

Costa, E. M. da. (2016). Sócio-Economia. In J. Rocha (Ed.), *Atlas Digital da Área Metropolitana de Lisboa*. Lisboa, Portugal: Centro de Estudos Geográficos.

Craft, C. B., Seneca, E. D., & Broome, S. W. (1991). Loss on ignition and kjeldahl digestion for estimating organic carbon and total nitrogen in estuarine marsh soils: Calibration with dry combustion. *Estuaries*, *14*(2), 175–179. doi:10.2307/1351691

Dare, S. A. S., Barnes, S.-J., Prichard, H. M., & Fisher, P. C. (2011). Chalcophile and platinum-group element (PGE) concentrations in the sulfide minerals from the

McCreedy East deposit, Sudbury, Canada, and the origin of PGE in pyrite. *Mineralium Deposita*, *46*(4), 381–407. doi:10.1007/s00126-011-0336-9

Dung, T. T. T., Cappuyns, V., Swennen, R., & Phung, N. K. (2013). From geochemical background determination to pollution assessment of heavy metals in sediments and soils. *Reviews in Environmental Science and Bio/Technology*, *12*(4), 335–353. doi:10.1007/s11157-013-9315-1

Eastin, J. A. (1991, April 10). Manufacturing and using nitrogen fertilizer solutions on a farm. Google Patents.

Ek, K. H., Morrison, G. M., & Rauch, S. (2004). Environmental routes for platinum group elements to biological materials--a review. *The Science of the total environment*, *334–335*, 21–38. doi:10.1016/j.scitotenv.2004.04.027

Ely, J. C., Neal, C. R., Kulpa, C. F., Schneegurt, M. A., Seidler, J. A., & Jain, J. C. (2001). Implications of Platinum-Group Element Accumulation along U.S. Roads from Catalytic-Converter Attrition. *Environmental Science & Technology*, *35*(19), 3816–3822. doi:10.1021/es001989s

Essumang, D. K., Dodoo, D. K., & Adokoh, C. K. (2008). The impact of vehicular fallout on the Pra estuary of Ghana (a case study of the impact of platinum group metals (PGMs) on the marine ecosystem). *Environmental Monitoring and Assessment*, *145*(1), 283–294. doi:10.1007/s10661-007-0037-0

European Commission. (1991). Council Directive 91/542/EEC of 1 October 1991 amending Directive 88/77/EEC on the approximation of the laws of the Member States relating to the measures to be taken against the emission of gaseous pollutants from diesel engines for use in vehicles. http://eur-lex.europa.eu/eli/dir/1991/542/oj. Accessed 22 January 2018

Folk, R. L. (1954). The Distinction between Grain Size and Mineral Composition in Sedimentary-Rock Nomenclature. *The Journal of Geology*, *62*(4), 344–359. doi:10.1086/626171

Fortunato, A. B., & Oliveira, A. (1999). On the effect of tidal flats on the hydrodynar6ics of the Tams estuarv, *22*, 31–44.

Fortunato, A., Oliveira, A., & Baptista, A. M. (1999). On the effect of tidal flats on the hydrodynamics of the Tagus estuary. *Oceanologica Acta*, *22*(1), 31–44. doi:https://doi.org/10.1016/S0399-1784(99)80030-9

Freire, P., Taborda, R., & Silva, A. (2007). Sedimentary characterization of Tagus estuarine beaches (Portugal). *Journal of Soils and Sediments*, *7*(5), 296–302. doi:10.1065/jss2007.08.243

Gaudêncio, M. J., Guerra, M. T., & Glémarec, M. (1991). Recherches biosédimentaires sur la zone maritime de l'estuaire du Tage, Portugal: données préliminaire. In M. Elliott & J.-P. Ducrotoy (Eds.), *Estuaries and Coasts: Spatial and Temporal Intercomparisons. ECSA 19 Symposium, Caen,* (pp. 11–16).

Gil, O., & Vale, C. (1999). DDT concentrations in surficial sediments of three estuarine systems in Portugal. *Aquatic Ecology*, *33*(3), 263–269. doi:10.1023/A:1009961901782

Hatfield, W. R., Beshty, B. S., Lee, H. C., Heck, R. M., & Hsiung, T. M. (1987,

636 November 11). Method for recovering platinum in a nitric acid plant. Google
637 Patents.

638 Haus, N., Eybe, T., Zimmermann, S., & Sures, B. (2009). Is microwave digestion using
639 TFM vessels a suitable preparation method for Pt determination in biological
640 samples by adsorptive cathodic stripping voltammetry? *Analytica chimica acta*,
641 *635*(1), 53–57. doi:10.1016/j.aca.2008.12.043

642 IMT. (2016). *Relatório de Tráfego na Rede Nacional de Autoestradas - 4º Trimestre*.
643 Lisboa, Portugal.

644 Jarvis, K. E., Parry, S. J., & Piper, J. M. (2001). Temporal and Spatial Studies of
645 Autocatalyst-Derived Platinum, Rhodium, and Palladium and Selected Vehicle-
646 Derived Trace Elements in the Environment. *Environmental Science &*
647 *Technology*, *35*(6), 1031–1036. doi:10.1021/es0001512

648 Kašpar, J., Fornasiero, P., & Hickey, N. (2003). Automotive catalytic converters:
649 current status and some perspectives. *Catalysis Today*, *77*(4), 419–449.
650 doi:https://doi.org/10.1016/S0920-5861(02)00384-X

651 Laschka, D., & Nachtwey, M. (1997). Platinum in municipal sewage treatment plants.
652 *Chemosphere*, *34*(8), 1803–1812. doi:http://dx.doi.org/10.1016/S0045-
653 6535(97)00036-2

654 Lemaire, A., Dournel, P., & Deschrijver, P. (2014, March 13). Process for the
655 manufacture of hydrogen peroxide. Google Patents.

656 Loring, D. H., & Rantala, R. T. T. (1992). Manual for the geochemical analyses of
657 marine sediments and suspended particulate matter. *Earth-Science Reviews*, *32*(4),
658 235–283. doi:https://doi.org/10.1016/0012-8252(92)90001-A

659 Mateus, M., & Neves, R. (2008). Evaluating light and nutrient limitation in the Tagus
660 estuary using a process-oriented ecological model. *Journal of Marine Engineering*
661 *& Technology*, *7*(2), 43–54. doi:10.1080/20464177.2008.11020213

662 Matys Grygar, T., & Popelka, J. (2016). Revisiting geochemical methods of
663 distinguishing natural concentrations and pollution by risk elements in fluvial
664 sediments. *Journal of Geochemical Exploration*, *170*, 39–57.
665 doi:http://dx.doi.org/10.1016/j.gexplo.2016.08.003

666 Mihaljevič, M., Galušková, I., Strnad, L., & Majer, V. (2013). Distribution of platinum
667 group elements in urban soils, comparison of historically different large cities
668 Prague and Ostrava, Czech Republic. *Journal of Geochemical Exploration*, *124*,
669 212–217. doi:https://doi.org/10.1016/j.gexplo.2012.10.008

670 Mil-Homens, M., Caetano, M., Costa, A. M., Lebreiro, S., Richter, T., de Stigter, H., et
671 al. (2013). Temporal evolution of lead isotope ratios in sediments of the Central
672 Portuguese Margin: A fingerprint of human activities. *Marine Pollution Bulletin*,
673 *74*(1), 274–284. doi:https://doi.org/10.1016/j.marpolbul.2013.06.044

674 Mil-Homens, M., Vale, C., Raimundo, J., Pereira, P., Brito, P., & Caetano, M. (2014).
675 Major factors influencing the elemental composition of surface estuarine
676 sediments: the case of 15 estuaries in Portugal. *Marine pollution bulletin*, *84*(1–2),
677 135–46. doi:10.1016/j.marpolbul.2014.05.026

678 Mil-Homens, M., Vicente, M., Grimalt, J. O., Micaelo, C., & Abrantes, F. (2016).

679 Reconstruction of organochlorine compound inputs in the Tagus Prodelta. *Science*
680 *of The Total Environment*, *540*, 231–240.
681 doi:https://doi.org/10.1016/j.scitotenv.2015.07.009

682 Miller, J., & Miller, J. (2010). *Statistics and chemometrics for analytical chemistry* (6th
683 ed.). Pearson Education Limited.

684 Moldovan, M., Palacios, M. A., Gómez, M. M., Morrison, G., Rauch, S., McLeod, C.,
685 et al. (2002). Environmental risk of particulate and soluble platinum group
686 elements released from gasoline and diesel engine catalytic converters. *Science of*
687 *The Total Environment*, *296*(1), 199–208. doi:https://doi.org/10.1016/S0048-
688 9697(02)00087-6

689 Monteiro, C. E., Cesário, R., O'Driscoll, N. J., Nogueira, M., Válega, M., Caetano, M.,
690 & Canário, J. (2016). Seasonal variation of methylmercury in sediment cores from
691 the Tagus Estuary (Portugal). *Marine Pollution Bulletin*, *104*(1), 162–170.
692 doi:https://doi.org/10.1016/j.marpolbul.2016.01.042

693 Monteiro, C. E., Cobelo-Garcia, A., Caetano, M., & Correia dos Santos, M. M. (2017).
694 Improved voltammetric method for simultaneous determination of Pt and Rh using
695 second derivative signal transformation – application to environmental samples.
696 *Talanta*, *175*, 1–8. doi:10.1016/j.talanta.2017.06.067

697 Nygren, O., Vaughan, G. T., Florence, T. M., Morrison, G. M., Warner, I. M., & Dale,
698 L. S. (1990). Determination of platinum in blood by adsorptive voltammetry.
699 *Analytical chemistry*, *62*(15), 1637–40. doi:10.1021/ac00214a020

700 Paparatto, G., De, A. G., D'aloisio, R., & Buzzoni, R. (2010, September 28). Catalyst
701 and its use in the synthesis of hydrogen peroxide. Google Patents.

702 Peucker-Ehrenbrink, B., & Jahn, B. (2001). Rhenium-osmium isotope systematics and
703 platinum group element concentrations: Loess and the upper continental crust.
704 *Geochemistry, Geophysics, Geosystems*, *2*(10), n/a-n/a.
705 doi:10.1029/2001GC000172

706 Prichard, H. M., & Fisher, P. C. (2012). Identification of Platinum and Palladium
707 Particles Emitted from Vehicles and Dispersed into the Surface Environment.
708 *Environmental Science & Technology*, *46*(6), 3149–3154. doi:10.1021/es203666h

709 Prichard, H. M., Jackson, M. T., & Sampson, J. (2008). Dispersal and accumulation of
710 Pt, Pd and Rh derived from a roundabout in Sheffield (UK): From stream to tidal
711 estuary. *Science of The Total Environment*, *401*(1), 90–99.
712 doi:https://doi.org/10.1016/j.scitotenv.2008.03.037

713 Prudêncio, M. I., Braga, M. A. S., & Gouveia, M. A. (1993). REE mobilization,
714 fractionation and precipitation during weathering of basalts. *Chemical Geology*,
715 *107*(3), 251–254. doi:https://doi.org/10.1016/0009-2541(93)90185-L

716 Rauch, S., Hemond, H. F., Barbante, C., Owari, M., Morrison, G. M., Peucker-
717 Ehrenbrink, B., & Wass, U. (2005). Importance of automobile exhaust catalyst
718 emissions for the deposition of platinum, palladium, and rhodium in the northern
719 hemisphere. *Environmental science & technology*, *39*(21), 8156–8162.

720 Rauch, S., Morrison, G. M., & Moldovan, M. (2002). Scanning laser ablation-ICP-MS
721 tracking of platinum group elements in urban particles. *Science of The Total*

Environment, *286*(1), 243–251. doi:https://doi.org/10.1016/S0048-9697(01)00988-3

Rauch, S., & Peucker-Ehrenbrink, B. (2015a). Sources of Platinum Group Elements in the Environment BT - Platinum Metals in the Environment. In F. Zereini & C. L. S. Wiseman (Eds.), (pp. 3–17). Berlin, Heidelberg: Springer Berlin Heidelberg. doi:10.1007/978-3-662-44559-4_1

Rauch, S., & Peucker-Ehrenbrink, B. (2015b). Sources of platinum group elements in the environment. In *Platinum metals in the environment* (pp. 3–17). Springer.

Rauch, S., Peucker-Ehrenbrink, B., Molina, L. T., Molina, M. J., Ramos, R., & Hemond, H. F. (2006). Platinum Group Elements in Airborne Particles in Mexico City. *Environmental Science & Technology*, *40*(24), 7554–7560. doi:10.1021/es061470h

Ravindra, K., Bencs, L., & Van Grieken, R. (2004). Platinum group elements in the environment and their health risk. *The Science of the total environment*, *318*(1–3), 1–43. doi:10.1016/S0048-9697(03)00372-3

Ruchter, N., & Sures, B. (2015). Distribution of platinum and other traffic related metals in sediments and clams (Corbicula sp.). *Water Research*, *70*, 313–324. doi:http://dx.doi.org/10.1016/j.watres.2014.12.011

Ruchter, N., Zimmermann, S., & Sures, B. (2015). Field studies on PGE in aquatic ecosystems. In *Platinum Metals in the Environment* (pp. 351–360). Springer.

Santos-Echeandía, J., Vale, C., Caetano, M., Pereira, P., & Prego, R. (2010). Effect of tidal flooding on metal distribution in pore waters of marsh sediments and its transport to water column (Tagus estuary, Portugal). *Marine environmental research*, *70*(5), 358–67. doi:10.1016/j.marenvres.2010.07.003

Schlitzer, R. (2017). Ocean Data View, odv.awi.de.

Sutherland, R. A., Pearson, G. D., Ottley, C. J., & Ziegler, A. D. (2015). Platinum-Group Elements in Urban Fluvial Bed Sediments—Hawaii. In *Platinum Metals in the Environment* (pp. 163–186). Springer.

Taborda, R., Freire, P., Silva, A., Andrade, C., & Freitas, M. (2009). Origin and evolution of Tagus estuarine beaches. *Journal of Coastal Research*, *SI*(56), 213–217.

Taylor, S. R., & McLennan, S. M. (1995). The geochemical evolution of the continental crust. *Reviews of Geophysics*, *33*(2), 241–265. doi:10.1029/95RG00262

Terashima, S., Katayama, H., & Itoh, S. (1993). Geochemical behavior of Pt and Pd in coastal marine sediments, southeastern margin of the Japan Sea. *Applied Geochemistry*, *8*(3), 265–271. doi:https://doi.org/10.1016/0883-2927(93)90041-E

Troupin, C., Barth, A., Sirjacobs, D., Ouberdous, M., Brankart, J.-M., Brasseur, P., et al. (2012). Generation of analysis and consistent error fields using the Data Interpolating Variational Analysis (DIVA). *Ocean Modelling*, *52–53*(Supplement C), 90–101. doi:https://doi.org/10.1016/j.ocemod.2012.05.002

Vale, C., Canário, J., Caetano, M., Lavrado, J., & Brito, P. (2008). Estimation of the anthropogenic fraction of elements in surface sediments of the Tagus Estuary

(Portugal). *Marine Pollution Bulletin*, *56*(7), 1364–1367. doi:https://doi.org/10.1016/j.marpolbul.2008.04.006

Vale, C., & Sundby, B. (1987). Suspended sediment fluctuations in the Tagus estuary on semi-diurnal and fortnightly time scales. *Estuarine, Coastal and Shelf Science*, *25*(5), 495–508. doi:http://dx.doi.org/10.1016/0272-7714(87)90110-7

Vaz, N., & Dias, J. M. (2014). Residual currents and transport pathways in the Tagus estuary, Portugal: the role of freshwater discharge and wind. *Journal of Coastal Research*, 610–615. doi:10.2112/SI70-103.1

Vaz, N., Mateus, M., & Dias, J. M. (2011). Semidiurnal and spring-neap variations in the Tagus Estuary : Application of a process-oriented hydro-biogeochemical model. *Journal of Coastal Research*, *SI*(64), 1619–1623.

Vyas, N., Turner, A., & Sewell, G. (2014). Platinum-based anticancer drugs in waste waters of a major UK hospital and predicted concentrations in recipient surface waters. *Science of The Total Environment*, *493*, 324–329. doi:https://doi.org/10.1016/j.scitotenv.2014.05.127

Wei, C., & Morrison, G. M. (1994). Platinum in road dusts and urban river sediments. *Science of The Total Environment*, *146–147*(Supplement C), 169–174. doi:https://doi.org/10.1016/0048-9697(94)90234-8

Wiseman, C. L. S., Hassan Pour, Z., & Zereini, F. (2016). Platinum group element and cerium concentrations in roadside environments in Toronto, Canada. *Chemosphere*, *145*, 61–67. doi:https://doi.org/10.1016/j.chemosphere.2015.11.056

Wiseman, C. L. S., & Zereini, F. (2009). Airborne particulate matter, platinum group elements and human health: a review of recent evidence. *The Science of the total environment*, *407*(8), 2493–2500. doi:10.1016/j.scitotenv.2008.12.057

Wiseman, C. L. S., Zereini, F., & Püttmann, W. (2013). Traffic-related trace element fate and uptake by plants cultivated in roadside soils in Toronto, Canada. *Science of The Total Environment*, *442*, 86–95. doi:https://doi.org/10.1016/j.scitotenv.2012.10.051

Zereini, F., Alt, F., Messerschmidt, J., von Bohlen, A., Liebl, K., & Püttmann, W. (2004). Concentration and Distribution of Platinum Group Elements (Pt, Pd, Rh) in Airborne Particulate Matter in Frankfurt am Main, Germany. *Environmental Science & Technology*, *38*(6), 1686–1692. doi:10.1021/es030127z

Zereini, F., & Wiseman, C. L. S. (2015). *Platinum Metals in the Environment*. (F. Zereini & C. L. S. Wiseman, Eds.). Berlin, Heidelberg: Springer Berlin Heidelberg. doi:10.1007/978-3-662-44559-4

Zereini, F., Wiseman, C., & Püttmann, W. (2007). Changes in Palladium, Platinum, and Rhodium Concentrations, and Their Spatial Distribution in Soils Along a Major Highway in Germany from 1994 to 2004. *Environmental Science & Technology*, *41*(2), 451–456. doi:10.1021/es061453s

Zhong, L., Yan, W., Li, J., Tu, X., Liu, B., & Xia, Z. (2012). Pt and Pd in sediments from the Pearl River Estuary, South China: background levels, distribution, and source. *Environmental Science and Pollution Research*, *19*(4), 1305–1314. doi:10.1007/s11356-011-0653-7

807

Caption of figures

Fig. 1 Map representation of the study area location, the Tagus estuary, SW Europe. Bathymetric data in meters (obtained from the Portuguese Hydrographic Institute; http://www.hidrografico.pt) with depicted stations where superficial sediments were collected (white dots); (**25A**) *25 de Abril* bridge; (**VG**) *Vasco da Gama* bridge (area in dashed line); *Industrialised areas* (**CN**, **LN**, **SN** and **BRR**, in circles); WWTP: (**A**) Alcântara, (**B**) Beirolas and (**C**) Chelas; and pluvial waters discharge (**TP**) Terreiro do Paço. Most relevant stations and the Natural Reserve area of the estuary are also indicated.

Fig. 2 Spatial distribution of Pt and Rh concentrations, in ng g^{-1}, in superficial sediments of Tagus estuary.

Fig. 3 Boxplot of (**a**) median and total concentrations (ng g^{-1}) of Pt and Rh in superficial sediments of Tagus estuary; (**b**) Pt and (**c**) Rh concentrations depicted by section, respectively; (**d**) Rh concentrations depicted in industry section. Significant differences amongst groups were observed (Kruskal-Wallis (H) test; $p<0.05$) and are indicated by different letters (Mann-Whitney (U) test; $p<0.05$).

Fig. 4 Bivariate plots between Pt and Rh with Al, LOI and Fe in superficial sediments of Tagus estuary. (●) *background* in the estuary; (●) *waste- and pluvial waters discharges*; (□) *VG bridge*; and (◇) *industrialised areas*. The dashed line represents the trends found in the background data and the Spearman correlations (r_S) found, respectively.

Fig. 5 Spatial distributions of Pt and Rh with concentrations normalised to Al, LOI and Fe in superficial sediments of Tagus estuary.

Fig. 6 (**a**) Pt and (**b**) Rh concentrations normalised to Al and LOI from WWTP discharge sites (**A**) Alcântara, (**B**) Beirolas and (**C**) Chelas, and pluvial- waters discharge site (**TP**) Terreiro do Paço, and respective control stations in superficial sediments from Tagus estuary: Alcântara upstream (A-U) and downstream (A -D); Beirolas upstream (B-U) and downstream (B -D), Chelas upstream (C-U) and downstream (C-D), and Terreiro do Paço upstream (TP-U) and downstream (TP -D). (*) Data not presented due to an outlier value of LOI.

Fig. 7 Signature of Pt and Rh in superficial sediments of Tagus estuary. The Pt/Rh range varied between 0.48 and 39, with the highest values found at BRR stations.

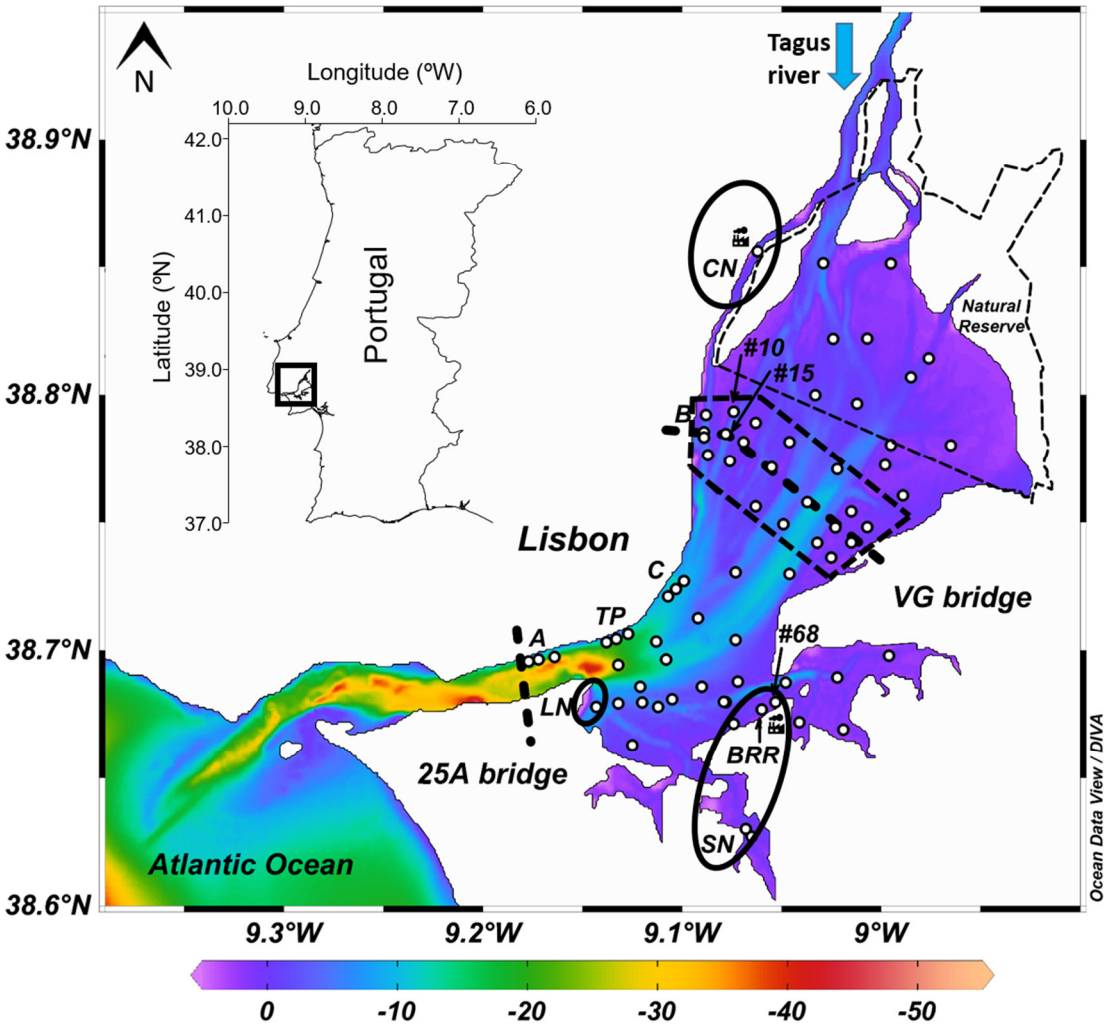
N
Longitude (ºW)
10.0
9.0
8.0
7.0
6.0
Latitude (ºN)
42.0
41.0
40.0
39.0
38.0
37.0
Portugal
Tagus river
CN
Natural Reserve
#10
#15
B
Lisbon
C
VG bridge
TP
A
#68
LM
BRR
SN
25A bridge
Atlantic Ocean
38.9°N
38.8°N
38.7°N
38.6°N
9.3°W
9.2°W
9.1°W
9°W
0
-10
-20
-30
-40
-50
Ocean Data View / DIVA

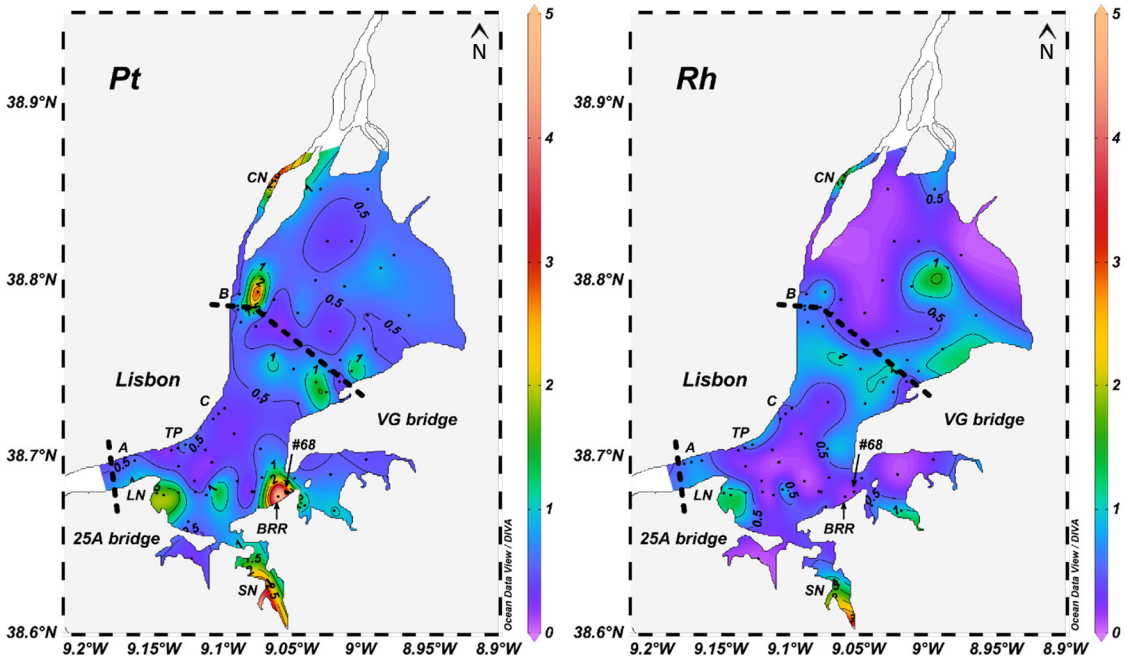
Pt
Rh
N
38.9°N
38.8°N
38.7°N
38.6°N
9.2°W
9.15°W
9.1°W
9.05°W
9°W
8.95°W
8.9°W
CN
B
C
TP
A
LN
#68
BRR
SN
Lisbon
VG bridge
25A bridge
Ocean Data View / DIVA
5
4
3
2
1
0

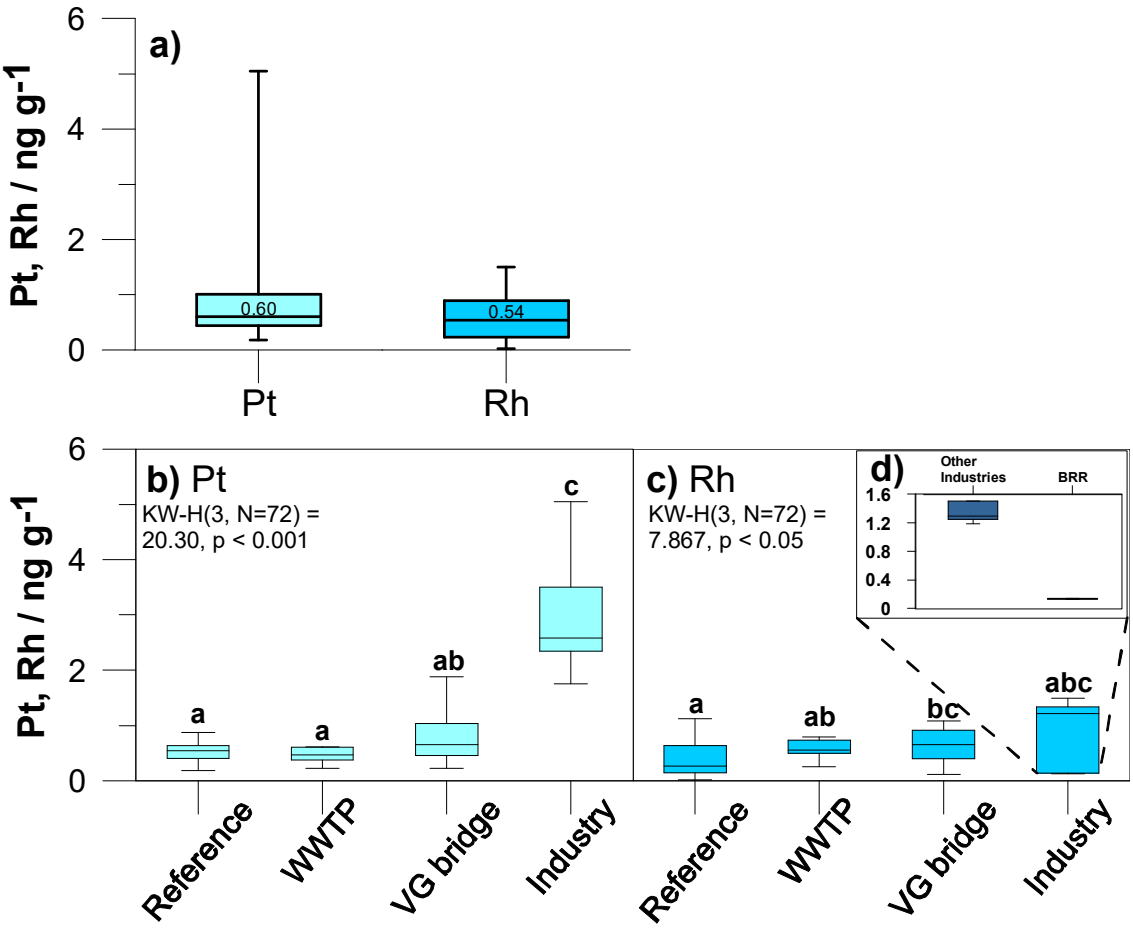
a)
Pt, Rh / ng g-1
6
4
2
0
0.60
0.54
Pt
Rh
b) Pt
KW-H(3, N=72) =
20.30, p < 0.001
c) Rh
KW-H(3, N=72) =
7.867, p < 0.05
d)
Other Industries
BRR
1.6
1.2
0.8
0.4
0
a
a
ab
c
a
ab
bc
abc
Reference
WWTP
VG bridge
Industry

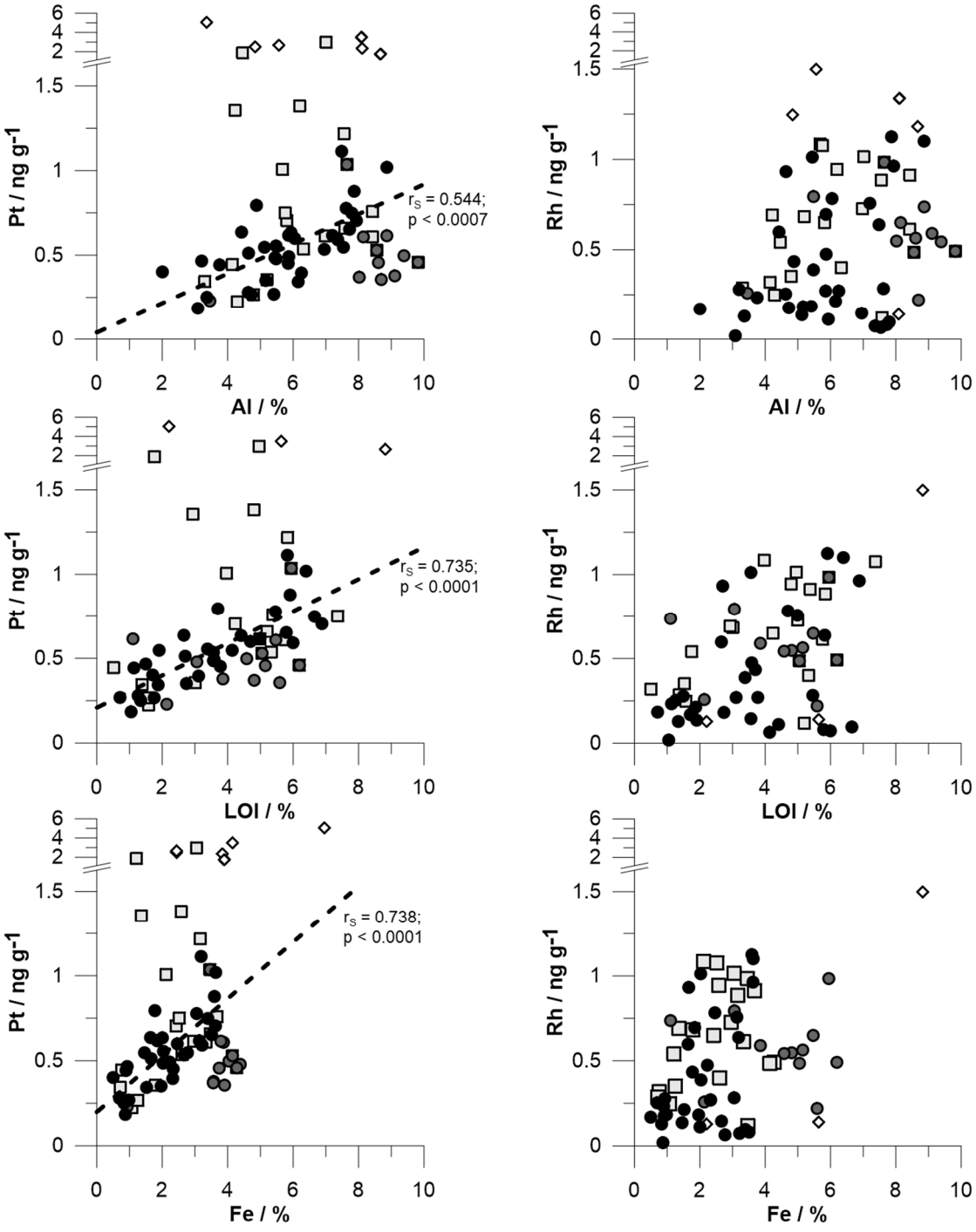
Pt / ng g-1
Rh / ng g-1
Al / %
LOI / %
Fe / %
rS = 0.544;
p < 0.0007
rS = 0.735;
p < 0.0001
rS = 0.738;
p < 0.0001

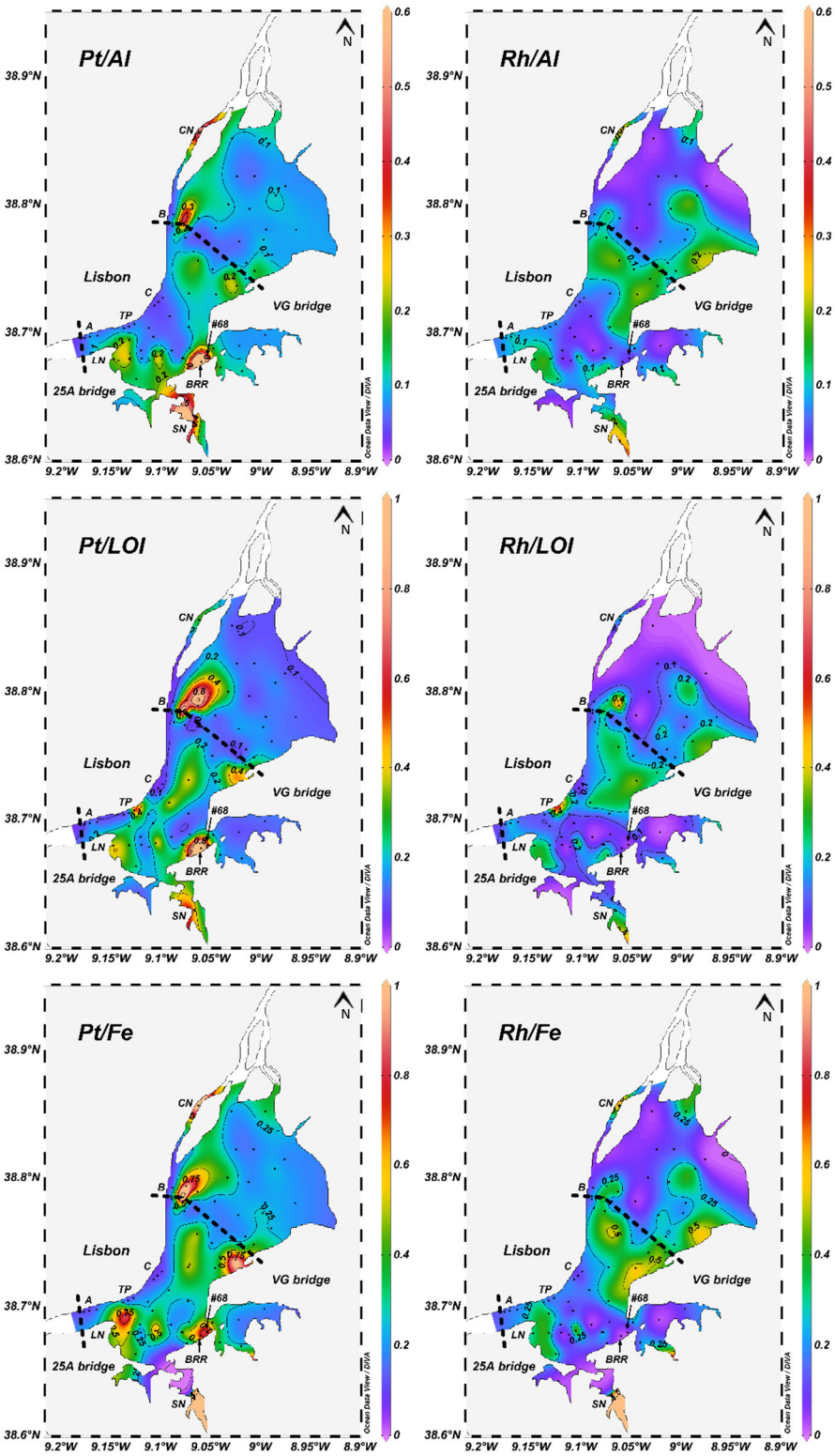
Pt/Al
Rh/Al
Pt/LOI
Rh/LOI
Pt/Fe
Rh/Fe
N
Lisbon
VG bridge
25A bridge
CN
B
C
TP
A
LN
#68
BRR
SN
38.9°N
38.8°N
38.7°N
38.6°N
9.2°W
9.15°W
9.1°W
9.05°W
9°W
8.95°W
8.9°W
Ocean Data View / DIVA

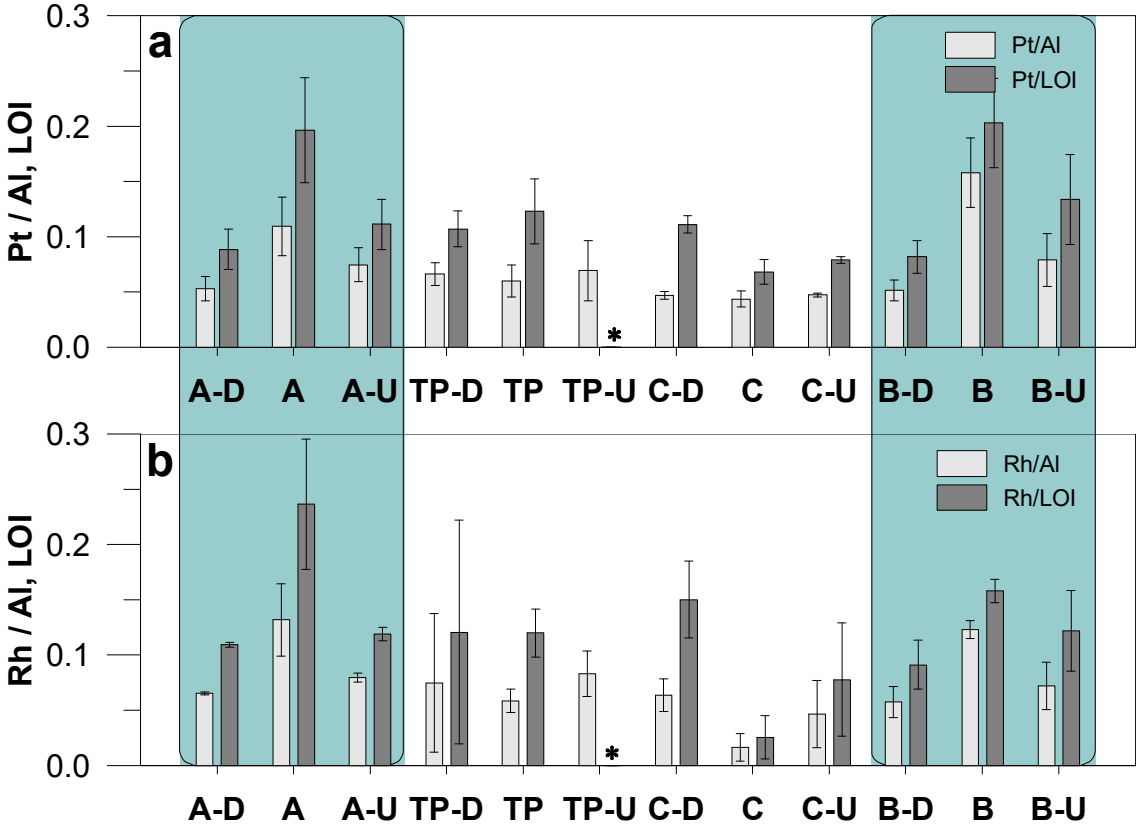
a
Pt/Al
Pt/LOI
Pt / Al, LOI
0.3
0.2
0.1
0.0
*
A-D
A
A-U
TP-D
TP
TP-U
C-D
C
C-U
B-D
B
B-U
b
Rh/Al
Rh/LOI
Rh / Al, LOI
0.3
0.2
0.1
0.0
*
A-D
A
A-U
TP-D
TP
TP-U
C-D
C
C-U
B-D
B
B-U

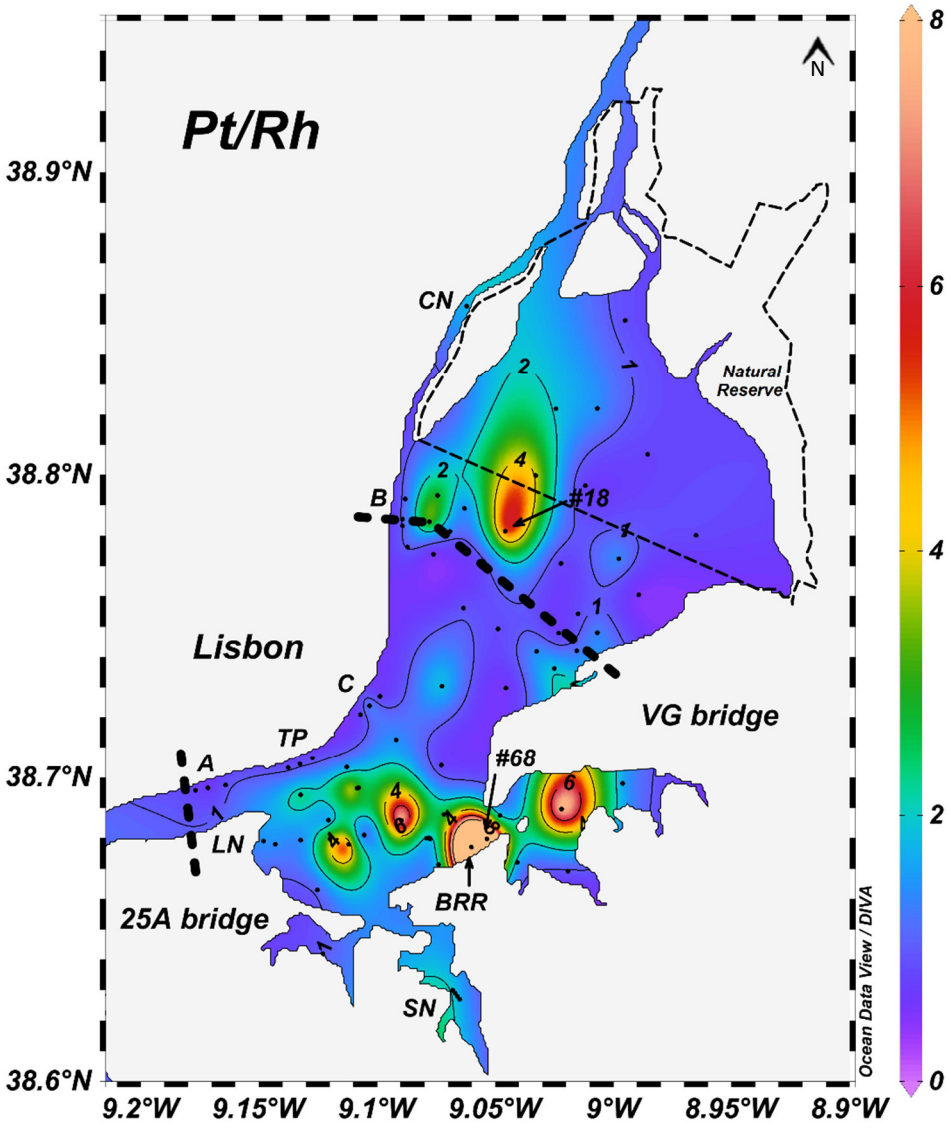
Pt/Rh
N
38.9°N
38.8°N
38.7°N
38.6°N
9.2°W
9.15°W
9.1°W
9.05°W
9°W
8.95°W
8.9°W
CN
Natural Reserve
B
#18
Lisbon
C
TP
A
LN
#68
VG bridge
BRR
25A bridge
SN
Ocean Data View / DIVA
8
6
4
2
0

Table 1 Descriptive statistics of the parameters used in the characterisation of the superficial sediments of Tagus estuary.

	Units	**n**	**Min**	**1st Quartile**	**Median**	**Mean**	**3rd Quartile**	**Max**
Al	%	72	2.0	4.8	6.0	6.2	7.7	9.8
Fe	%	72	0.50	1.6	2.5	2.6	3.6	7.0
Mn	%	70	0.010	0.023	0.030	0.033	0.041	0.71
Mg	%	70	0.16	0.49	0.80	0.76	1.0	1.4
Ca	%	70	0.01	0.49	1.2	1.7	2.5	7.1
Sand	%	57	2.4	15	41	42	64	98
Silt + Clay	%	57	2.1	34	59	57	85	98
LOI	%	72	0.51	2.2	3.9	3.9	5.4	8.8

SUPPORTING INFORMATION

Platinum and Rhodium in Tagus Estuary, SW Europe: sources and spatial distribution

Carlos Eduardo Monteiro[1,2*], Margarida Correia dos Santos[2], Antonio Cobelo-Garcia[3], Pedro Brito[1] and Miguel Caetano[1]

[1] IPMA—Portuguese Institute of Sea and Atmosphere, Division of Oceanography and Marine Environment, Av. Brasília, 1449-006 Lisbon, Portugal

[2] Environmental Biogeochemistry, Centro de Química Estrutural, Instituto Superior Técnico, Universidade de Lisboa, Av. Rovisco Pais 1, 1049-001, Lisboa, Portugal

[3] Bioxeoquímica Mariña, Instituto de Investigacións Mariñas IIM-CSIC, Eduardo Cabello 6, 36208 Vigo, Pontevedra, Spain

*Corresponding author: Carlos E. Monteiro:
carlos.monteiro@ipma.pt
carlos.e.monteiro@tecnico.ulisboa.pt

IPMA—Instituto português do Mar e da Atmosfera, Divisão de Oceanografia e Ambiente Marinho,
Av. Brasília, 1449-006 Lisboa, Portugal

+351 218 447 000

Centro de Química Estrutural, Instituto Superior Técnico, Universidade de Lisboa, Av. Rovisco Pais 1, Torre Sul Lab 11.6-2, 1049-001, Lisboa, Portugal

+351 218 419 177

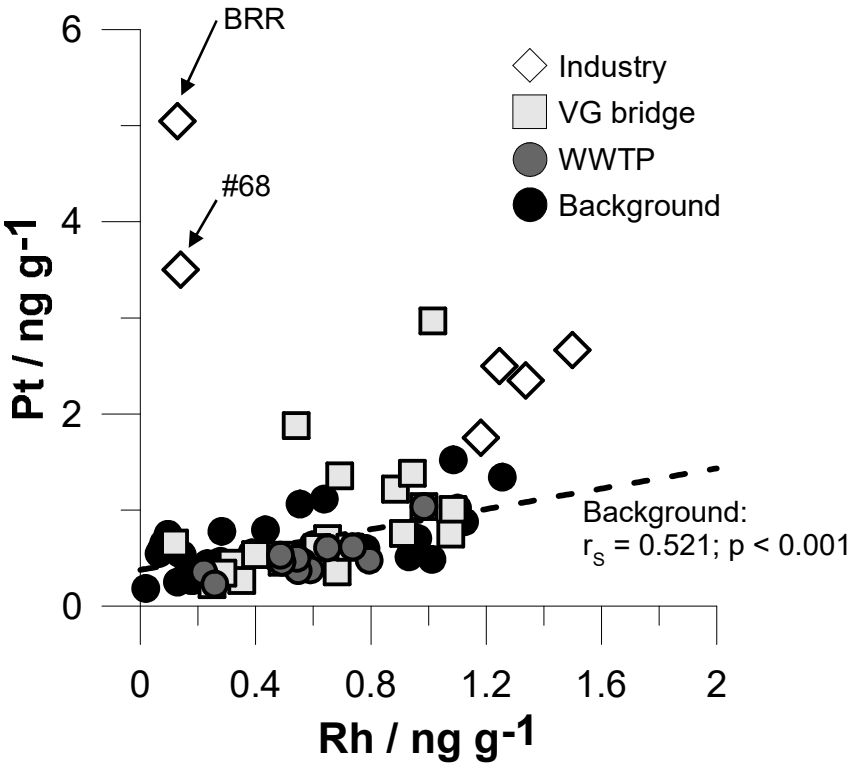

S.I. Fig. 1 Bivariate plot of Pt and Rh in superficial sediments of Tagus estuary, depicted by section; trend on the background data and the respective Spearman correlation (r_S) are represented by the dashed line.

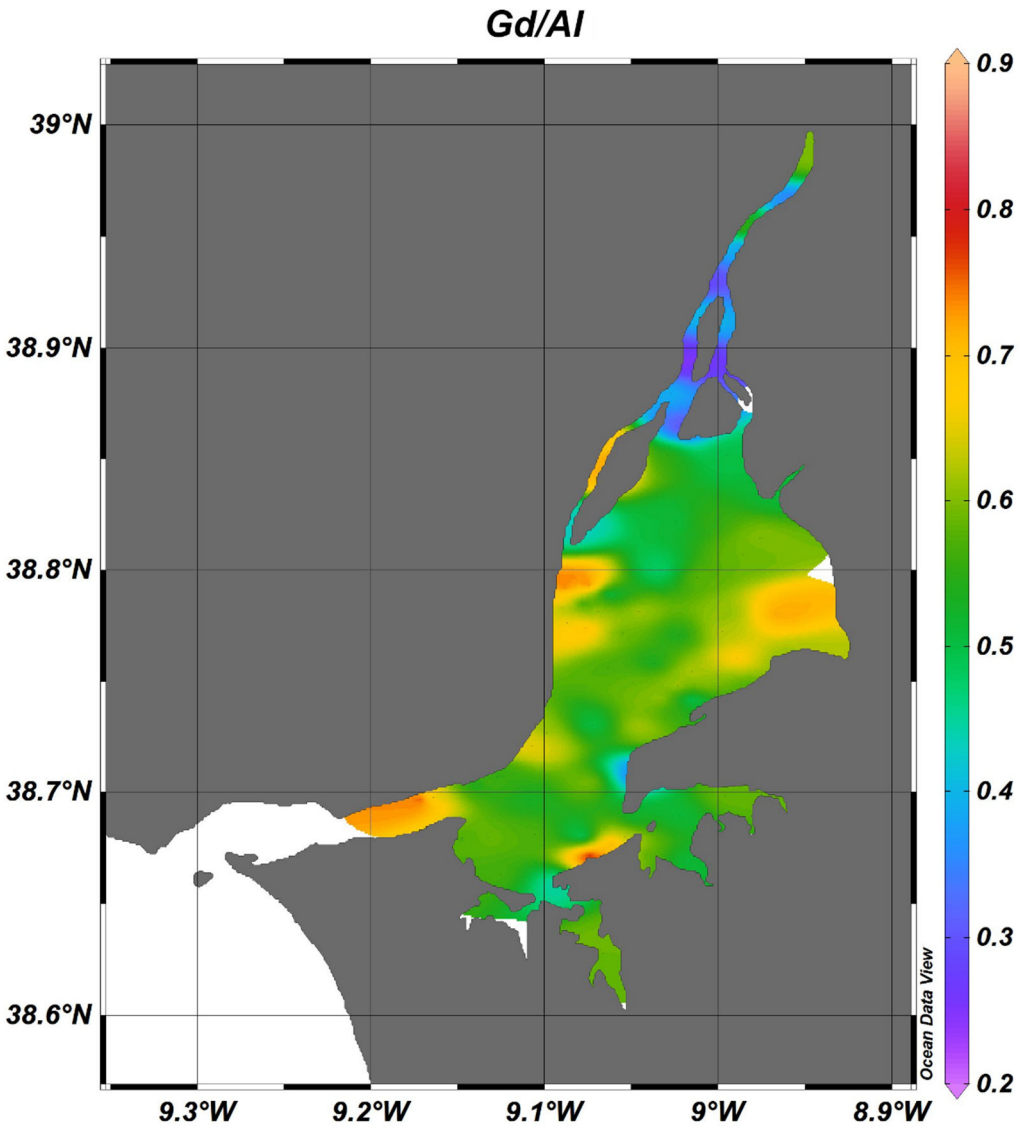

S.I. Fig. 2 Spatial distribution of Gd concentrations normalised to Al in superficial sediments of Tagus estuary.

Estimation of Pt and Rh emissions

Using the same approach as in Almécija et al. (2015), we estimated the range of Pt and Rh emissions from ACC in VG and 25A bridges. Table A.1 summarises the calculations based on: (i) minimum and maximum number of vehicles per day crossing the bridges in one year period (2015/2016) before the sampling (IMT 2016); (ii) the deck lengths: 17.2 km long for VG bridge and 2.3 km for 25A bridge (www.lusoponte.pt); (iii) the proportion of gasoline engine vehicles to diesel engine that is approximately 4:6 (ACEA 2017); (iv) the range of estimated release of Pt and Rh from ACC at a rate of ng km^{-1} (Palacios et al. 2000); and (v) the number of days calculated since the opening of VG bridge until the sampling campaign (6631 days), as well as for 25A bridge for comparison purposes. Almécija et al. (2015) has estimated that nearly 450 and 1140 g of Pt has been released over 13 years since the opening of VG bridge, using two different approaches. Our estimation of total emissions ranged from 542 – 937 g of Pt and 130 – 262 g of Rh in VG bridge, while for 25A bridge were 171 – 312 g of Pt and 41 – 87 g of Rh, since the opening of VG bridge in 1998.

Table A.1 - Estimation of Pt and Rh range of emissions in *Vasco da Gama* (VG) bridge and *25 de Abril* (25A) bridge since the opening of VG bridge.

***Vasco da Gama* (VG) bridge**			
Beginning of activity	April 1998		
Sampling for this work	June 2016		
Estimated number of days		6631	
Vehicles traffic / day - 1 year previous to sampling			
	min	53264	
	max	61353	
Extension of the bridge		17.2	km
***25 de Abril* (25A) bridge**			

Beginning of activity		previous to 1990		
Sampling for this work		June 2016		
Estimated number of days		9125		
Vehicles traffic / day - 1 year previous to sampling				
	min	125649		
	max	152957		
Extension of the bridge		2.3	km	
For comparison purposes, nº days in calculations: 6631				
Diesel vehicles[a]	65	%		
Petrol vehicles[a]	35	%		
New vehicles[a]	7	%		
Old vehicles[a]	93	%		

Estimated range of Pt emissions[b]

		min		max
Petrol				
New vehicles	ng M /km	102		
Old vehicles	ng M /km	6.3	-	8.2
Diesel				
New vehicles	ng M /km	404	-	812
Old vehicles	ng M /km	110	-	152
VG bridge TOTAL	**g Pt**	**542**	-	**937**
25A bridge TOTAL	**g Pt**	**171**	-	**312**

Estimated range of Rh emissions[b]

		min		max
Petrol				
New vehicles	ng M /km	38	-	66
Old vehicles	ng M /km	3.7	-	12
Diesel				
New vehicles	ng M /km	82	-	184
Old vehicles	ng M /km	26	-	39
VG bridge TOTAL	**g Rh**	**130**	-	**262**

25A bridge TOTAL	**g Rh**	**41 - 87**	

[a] Estimated from Instituto Nacional de Estatística and http://www.acea.be/statistics/
[b] Estimated emissions of Pt and Rh according to Palacios et al. (2000) and Almécija et al. (2015).

References

ACEA. (2017). *Vehicles in use - Europe 2017*. Brussels, Belgium.

Almécija, C., Sharma, M., Cobelo-García, A., Santos-Echeandía, J., & Caetano, M. (2015). Osmium and platinum decoupling in the environment: Evidences in intertidal sediments (Tagus Estuary, SW Europe). *Environmental Science and Technology*, *49*(11), 6545–6553. doi:10.1021/acs.est.5b00591

IMT. (2016). *Relatório de Tráfego na Rede Nacional de Autoestradas - 4º Trimestre*. Lisboa, Portugal.

Palacios, M. A., Gómez, M. M., Moldovan, M., Morrison, G., Rauch, S., McLeod, C., et al. (2000). Platinum-group elements: quantification in collected exhaust fumes and studies of catalyst surfaces. *Science of The Total Environment*, *257*(1), 1–15. doi:https://doi.org/10.1016/S0048-9697(00)00464-2